Research Article

Xuedan Dong, Aiqin Wang*, Jingpei Xie, and Zhen Wang

Optimization of volume fraction and microstructure evolution during thermal deformation of nano-SiCp/Al–7Si composites

https://doi.org/10.1515/ntrev-2021-0088
received July 7, 2021; accepted September 10, 2021

Abstract: This paper takes nano-SiCp/Al–7Si matrix composites prepared by powder metallurgy as the research object. With the help of advanced microstructure characterization techniques and performance analysis methods, the effect of nano-SiCp volume fraction on the microstructure and properties of composites is systematically studied. Based on optimizing the volume fraction of nano-SiCp, the thermal deformation behavior of the composites is investigated. It was found that with an increase of nano-SiCp content, the distribution uniformity of nano-SiCp decreases gradually. And because the surface of nano-SiCp is easy to adsorb gas and the aggregated distribution of nano-SiCp is not conducive to the sintering process, the density of the composites shows a gradually decreasing trend. The hardness of the composites tends increasing gradually, and the increase in amplitude gradually decreases. Due to the addition of nano-SiCp, there are many interfaces between SiCp and Al matrix, and cracks are prone to initiation and expansion at the interface. Therefore, as the volume fraction of nano-SiCp increases, the elongation of nano-SiCp/Al–7Si composites gradually decreases. When the volume fraction of nano-SiCp is 2%, the strength of the composites reaches the maximum value of 217 MPa. Compared with the Al–Si alloy without adding nano-SiCp, the results increased by 37.3%. In addition, with the decrease of strain rate and the increase of deformation temperature, the dislocation density in the composites gradually decreases, and the dynamic softening progresses more fully. The dynamic recrystallization nucleation mechanism mainly includes the subcrystal merging mechanism and the grain boundary bowing mechanism.

Keywords: nano-SiCp/Al–7Si composites, volume fraction, microstructure, performance

1 Introduction

With the rapid development of modern industry, the traditional single metal material has been far from meeting the requirements of modern industry on the performance of materials, so metal matrix composites came into being [1,2]. Among many metal matrix composites, SiCp/Al composites are widely used in aerospace, electronic packaging, and automobile fields because of their low thermal expansion coefficient, high strength, good wear resistance, and other advantages [3–5]. The traditional SiCp/Al composites are strengthened by micron-sized SiCp as the reinforcing material. Mao *et al.* [6] prepared aluminum matrix composites (AMCs) with SiCp volume fractions of 2.5 and 5% by powder metallurgy and studied the effect of SiCp volume fraction on microstructure and properties of composites. The results show that with the increase of SiCp volume fraction, the grain size of the composites decreases, the dislocation strengthening increases, and the strength and hardness are significantly improved. Wang *et al.* [7] analyzed the effects of different SiCp sizes on the microstructure and properties of 6061 Al matrix composites. This study indicated that, with the increase of SiCp size, the SiCp distributed more uniformly in the matrix and the coefficient of thermal expansion of composites increased, but the tensile strength of composites decreased. Although the addition of micron-sized SiCp to the matrix material can achieve a significant strengthening effect, a large number of studies have shown that the micron-sized SiCp can significantly reduce the plasticity of the matrix material while strengthening the matrix material, so that the application of SiCp/Al composites in the industrial field is limited [8,9].

* **Corresponding author: Aiqin Wang,** School of Materials Science and Engineering, Henan University of Science and Technology, Luoyang 471023, China, e-mail: aiqin_wang888@163.com
Xuedan Dong, Zhen Wang: School of Materials Science and Engineering, Henan University of Science and Technology, Luoyang 471023, China
Jingpei Xie: Collaborative Innovation Center of Non-Ferrous Materials of Henan Province, Luoyang 471023, China

To solve this problem, the researchers considered nano-SiCp/Al composites. Compared with micron-sized SiCp, the bonding area between nano-SiCp and the substrate with the same volume fraction is larger, which can better restrain the deformation of the substrate. At the same time, the particle spacing of nano-SiCp is smaller, which is conducive to the dispersion strengthening of SiCp. Therefore, nano-SiCp/Al composites are expected to obtain better strengthening effects [10]. Some recent studies have shown that while improving the strength of the matrix, the plasticity of nano-SiCp is slightly lower than that of the matrix or even equivalent to that of the matrix [11–13]. Its excellent comprehensive properties have aroused the interest of a large number of researchers, making nano-SiCp/Al composites a research hotspot. Zhang *et al.* [14] fabricated nano-SiCp/2014Al composites by semi-solid stir casting combined with hot extrusion and investigated the tensile properties at elevated temperatures of composites. The results show that nano-SiCp can remarkably improve the tensile strength at 493 K of Al2014 alloy without sacrificing the ductility, and the strengthening effect for the matrix alloy of 0.5 vol% nano-particles is superior to that of 4 vol% micron-particles. Hu *et al.* [15] prepared SiCp/A356 composites with different SiCp mass fractions by ultrasonic treatment, and the effects of nano-SiCp content on the microstructure and mechanical properties of the composites were investigated. The results show that the microstructure is obviously refined, and nano-SiCp is distributed uniformly around the eutectic Si by ultrasonic treatment. The ultimate tensile strength, yield strength, and elongation of the 0.5, 1, and 2% SiCp/A356 nanocomposites are simultaneously improved, respectively. Especially, when the SiCp content is 2%, the mechanical properties of composites reach the best. Kamrani *et al.* [16] produced Al (1, 3, 5, 7, 10 vol%) SiC nanocomposites by mechanical alloying (MA) and double pressing/sintering route and the effect of SiCp volume fraction on the mechanical properties of Al–SiC nanocomposites. It was shown that with the increase of SiC volume fraction, the grain size of the composite decreases gradually, and the mechanical properties are improved.

In the practical application of SiCp/Al composites, SiCp/Al composites usually need to undergo secondary thermal processing deformation to eliminate structural defects in the composites and optimize the distribution of SiCp, thereby improving the performance of SiCp/Al composites. And different thermal deformation process parameters will have a significant impact on the microstructure and properties, so it is necessary to study the microstructure and properties of the composites after deformation by different deformation process parameters [17–21]. At present, most of the researches on nano-SiCp/Al matrix composites are made by the casting method, while the thermal deformation behavior of SiCp/Al–Si composites prepared by the powder metallurgy method is still lack of systematic research. In this study, nano-SiCp/Al–7Si composites prepared by the powder metallurgy method were used as the research object. With the help of advanced microstructure characterization technology and property analysis method, the influence of nano-SiCp volume fraction on the thermal deformation process and microstructure evolution of composites was systematically studied. It is expected to provide a theoretical basis and data support for the optimization of composite volume fraction and the selection of hot deformation process parameters.

2 Materials and methods

In this experiment, Al–7Si alloy powder with a median diameter of 8 μm was selected as the matrix, and SiCp with a median diameter of 80 nm was used as the reinforcement. The SiCp/Al–7Si composites were prepared by powder metallurgy. Table 1 shows the chemical composition of the original Al–Si powder. The powders were mixed by a high-energy ball milling method using the QM-BP planetary ball mill at a ball milling speed of 150 rpm for 20 h. The mixture was then pressed by YD32 four-pillar hydraulic machine at a pressure of 500 MPa for 45 min, and the samples were sintered in a KSS-1200 tube furnace at 550°C for 4 h. The heating rate was 3°C min^{-1}. The sintered body was hot extruded using an XJ-500 extruder at 480°C with an extrusion speed of 1 mm s^{-1}. Then, the nano-SiCp/Al–Si composites were annealed in SX22-510 resistance furnace at 300°C for 2 h and then cooled to room temperature in the furnace.

JEM-2100 transmission electron microscope, JSM-5610LV scanning electron microscope, and Olympus PMG3 microscope were used to observe the microstructure of the materials. The sample needs to be corroded before microstructure observation. The corroder used is Keller reagent, and the ratio of mixed acid composition is 95 mL H_2O + 2.5 mL HNO_3 + 1.5 mL HCL + 1 mL HF. The preparation method of the TEM samples was to first cut the material into a thin slice with a thickness of 0.3 mm and then manually

Table 1: Chemical composition of original Al–Si powder (wt%)

Si	Mg	Fe	Al
7	0.3	0.1	Bal.

polished the slice to a thickness of about 50 μm with sandpaper. Next, it was punched into thin slices with a diameter of 3 mm and finally thinned on the Gatan-691 ion thinner. The mechanical properties of the materials were measured by an Ag-1250kN tensile testing machine and an HVS-1000A hardness tester. The nano-SiCp/Al–7Si composites of optimal volume fraction were machined into small cylindrical samples with a diameter of 10 mm and a height of 15 mm by wire cutting, and a 0.5 mm × 2 mm hole for installing a thermocouple was drilled into the side of the sample. Subsequently, the thermal compression test was conducted on the nano-SiCp/Al–Si composites using a Gleeble-1500D thermal simulator at 470, 490, 510, and 530°C and strain rates of 0.01, 0.1, 1, and 5 s^{-1}.

3 Results and discussion

3.1 Metallographic diagram of SiCp/Al–7Si matrix composites

As can be seen from Figure 1, the size of the silicon phase does not change significantly with the increase of the content of nano-SiC particles. However, studies have shown that the addition of nano-SiCp can improve the morphology of the Si phase and refine the Si particles in the Al-matrix composites prepared by the casting method [22]. This may be because the preparation temperature required by the powder metallurgy method is lower than that of the casting method, and the silicon phase is not generated by heterogeneous nucleation with nano-SiCp as the substrate in the liquid phase. No nano-SiC particles were observed in the metallographic diagram. This is because the distribution of nano-SiCp could not be observed with the low magnification of a metallographic microscope. Therefore, transmission electron microscopy with higher magnification was needed to observe the distribution of nano-SiCp.

Figure 2 shows the SEM images of the composites with different nano-SiCp contents. The black and sharp-edged phase in the picture is the nano-SiC phase. When the volume fraction of nano-SiCp is low, there is no obvious hole defect, indicating that the composite material has a better preparation effect. When the nano-SiCp addition amount is 4%, the microscopic pores increase significantly. On the one hand, it may be due to the larger specific surface energy of nano-SiCp particles [23]. As the content of nano-SiCp increases, the gas adsorbed on the surface of SiCp gradually increases. During the sintering process, the gas adsorbed on the surface of the nano-particles is discharged, leaving more porous holes in the composite material. On the other hand, the higher

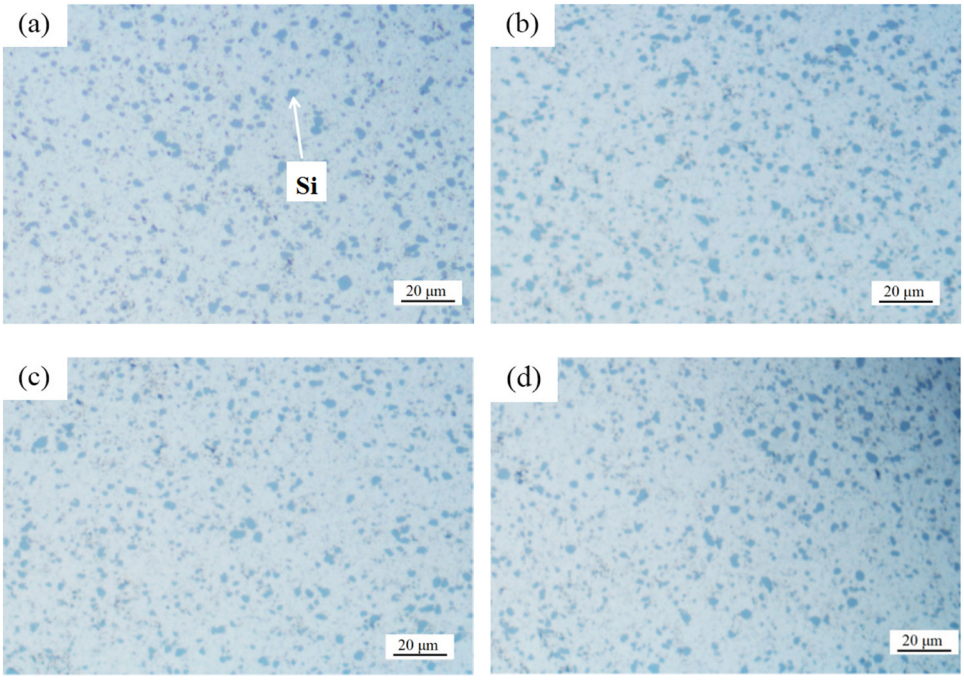

Figure 1: Metallographic structure of composites with different nano-SiCp volume fraction: (a) 1% SiCp, (b) 2% SiCp, (c) 3% SiCp, and (d) 4% SiCp.

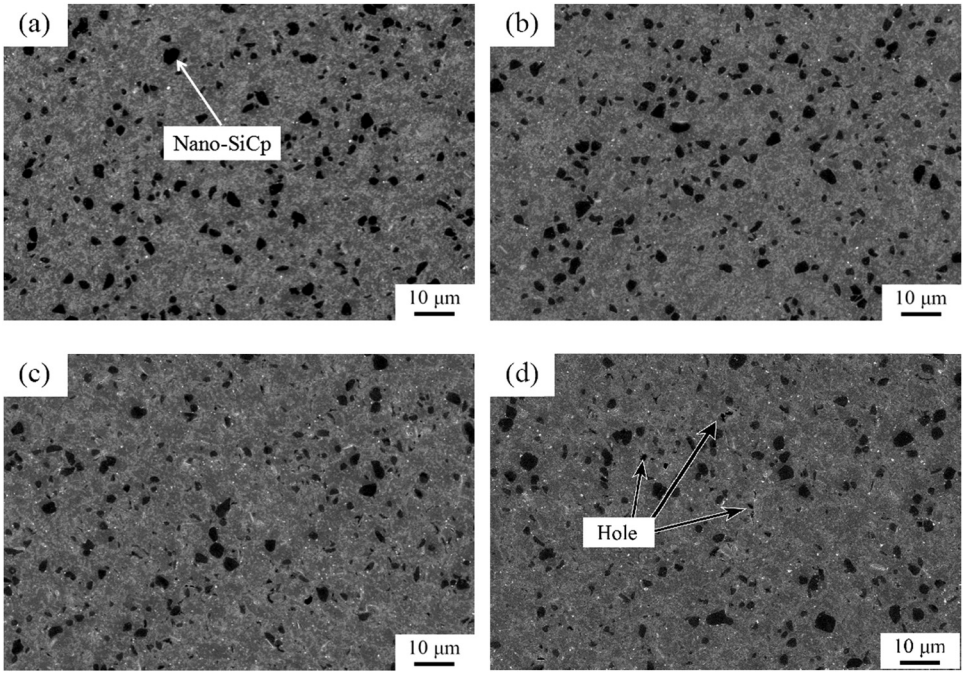

Figure 2: SEM images of composites with different nano-SiCp volume fraction: (a) 1% SiCp, (b) 2% SiCp, (c) 3% SiCp, and (d) 4% SiCp.

the content of nano-SiCp, the greater the possibility of nano-SiCp aggregation. The agglomerated distribution of nano-SiCp increases the resistance of atomic diffusion during sintering, which is not conducive to the sintering process, thereby leaving holes in the material [24].

Figure 3 is the TEM images of nano-SiCp/Al–7Si matrix composites with different SiCp contents. Figures 3e and f are the diffraction patterns of SiC and precipitate Al_4Cu_9, respectively. As can be seen from the TEM images, when the content of nano-SiCp is low, the distribution of nano-SiCp is better, and the spacing between particles is more uniform, no obvious aggregation phenomenon. When the content of nano-SiCp is more than 2%, the particle spacing between nano-SiC particles becomes shorter, and the dispersion of particles in some areas decreases. When the addition amount is 4%, the dispersion of nano-SiCp is poor, and some nano-SiCp have an aggregation phenomenon.

In addition, it can be noted that in Figure 3d, a large number of dislocations are distributed around nano-SiC particles, which may be due to the mismatch of the thermal expansion capacity between nano-SiC particles and the matrix, and there is a difference in the shrinkage of the nano-SiC particles and the adjacent aluminum matrix during the preparation and quenching process. As a result, thermal mismatch stress is generated around nano-SiC particles, and the thermal mismatch stress causes thermal strain in the matrix near nano-SiC particles, thus forming a large number of dislocations around nano-SiC particles [25].

3.2 Properties of nano-SiCp/Al–7Si matrix composites

Table 2 shows the relative density of nano-SiCp/Al–7Si composites with different SiCp contents. As can be seen from the table, the density of the composites is high, and when the content of nano-SiCp increases, the density of nano-SiCp/Al–7Si matrix composites has a trend of gradual decrease, which may be because nano-SiC particles have larger specific surface energy and easy to adsorb gas. In the process of sintering, the gas adsorbed on the surface of nanoparticles is discharged and holes are left in the composites. The higher the content of nano-SiCp, the more holes are contained in the composites, and the existence of holes reduces the density of the composites. In addition, the TEM observation results show that with the increase of the volume fraction of nano-SiCp, the distribution uniformity of nano-SiCp decreases gradually. The agglomerated distribution of nano-SiCp increases the resistance of atomic diffusion in the sintering process, which is not conducive to sintering. Therefore, the higher the content of nano-SiCp, the more difficult the sintering, and the lower the density of the composites.

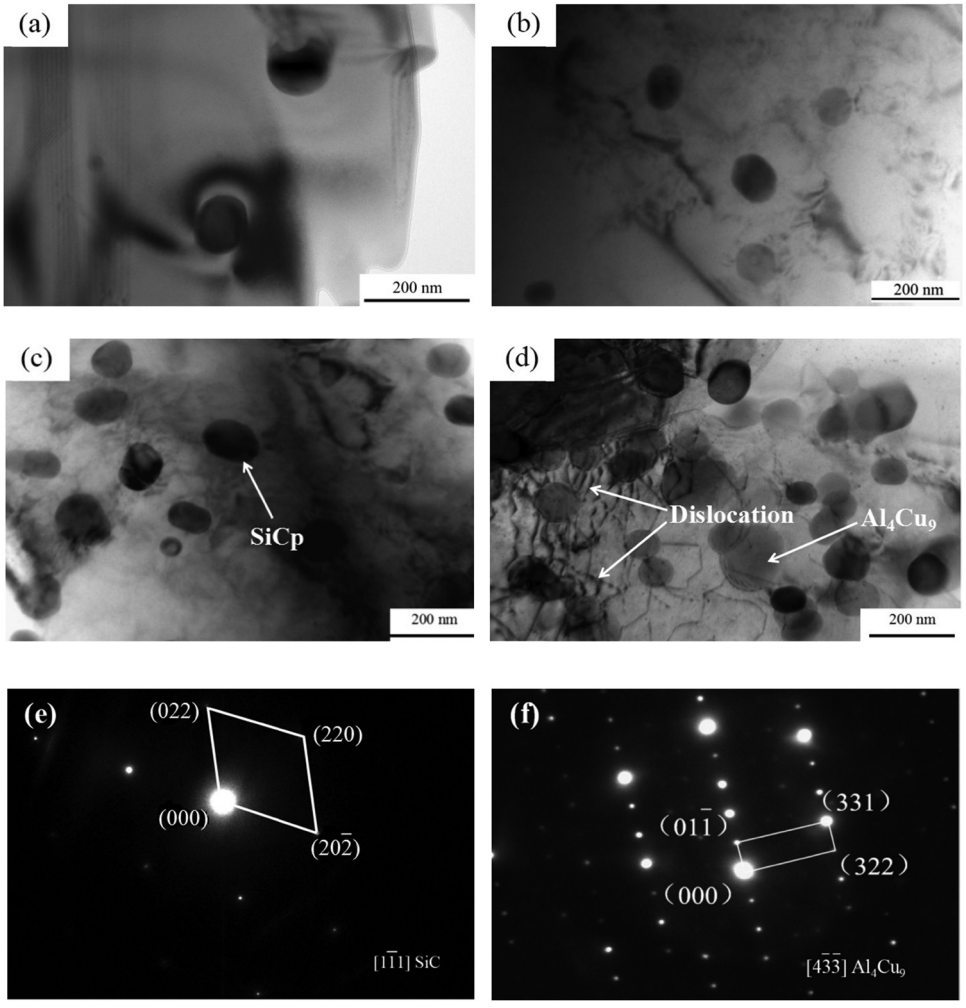

Figure 3: TEM images of composites with different nano-SiCp volume fraction: (a) 1% SiCp, (b) 2% SiCp, (c) 3% SiCp, (d) 4% SiCp, (e) diffraction patterns of SiC, and (f) diffraction patterns of Al_4Cu_9.

The hardness of nano-SiCp/Al–7Si matrix composites with different SiCp contents is shown in Figure 4. It can be seen that with the increase of the content of nano-SiCp, the hardness of the composites gradually increases, but the increased amplitude gradually decreases. This may be because when the volume fraction of nano-SiCp is low, the distribution of nano-SiCp in the material is more uniform, which can effectively restrain the deformation of the matrix, thereby significantly increasing the hardness of the material. However, when the addition amount of nano-SiCp is relatively high, part of SiC particles will agglomerate, which reduces the effective nano-SiC particles that have a strengthening effect. Moreover, according to the previous analysis, it is known that when

Table 2: Relative density of nano-SiCp/Al–7Si composites with different SiCp volume fraction

Nano-SiCp content (%)	Dry weight (g)	Wet weight (g)			Average wet weight (g)	Measured density (g cm^{-3})	Theoretical density (g cm^{-3})	Relative density (%)
0	9.9810	6.2560	6.2530	6.2545	6.2545	2.6784	2.7000	99.2
1	9.9071	6.2030	6.2040	6.2035	6.2035	2.6750	2.7051	98.9
2	10.0732	6.3150	6.3030	6.3090	6.3090	2.6761	2.7102	98.7
3	9.9181	6.2050	6.2030	6.2040	6.2040	2.6704	2.7153	98.3
4	9.8749	6.1850	6.1660	6.1755	6.1755	2.6693	2.7204	98.1

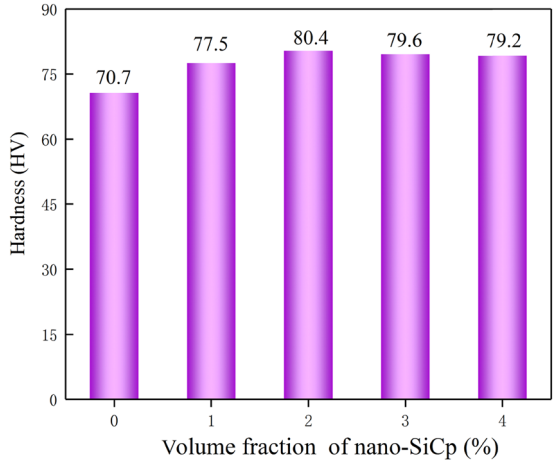

Figure 4: Hardness of nanocomposites with different SiCp volume fractions.

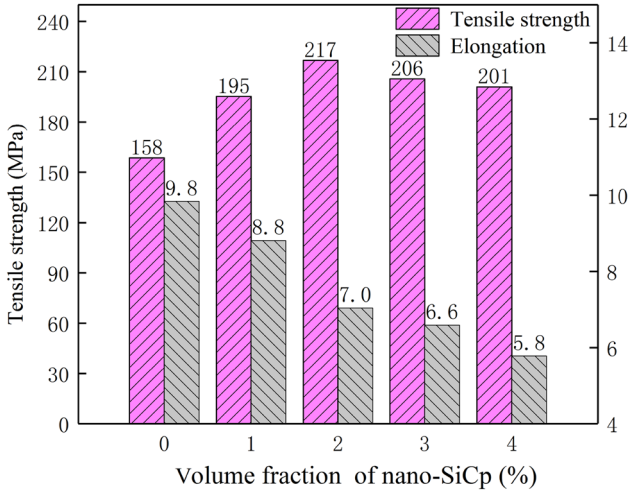

Figure 6: Tensile properties of nanocomposites with different SiCp volume fractions.

the nano-SiCp agglomerates, the density of the composites will decrease and the internal structure becomes loose. Therefore, the increased amplitude of hardness of the composites reduces.

The engineering stress-strain curve of the nano-SiCp/Al–7Si composites with different SiCp volume fractions is shown in Figure 5, and the results of tensile tests are summarized in Figure 6. As can be seen from the figure, with the increase of nano-SiCp addition amount, the strength of the composites increases first and then decreases. This is because when the addition amount of nano-SiCp is small, nano-SiC particles can not only hinder the slip of the dislocation but also induce the initiation of a large number of dislocations in the matrix due to the great difference between the thermal expansion coefficient and the elastic modulus and the matrix, to strengthen the material

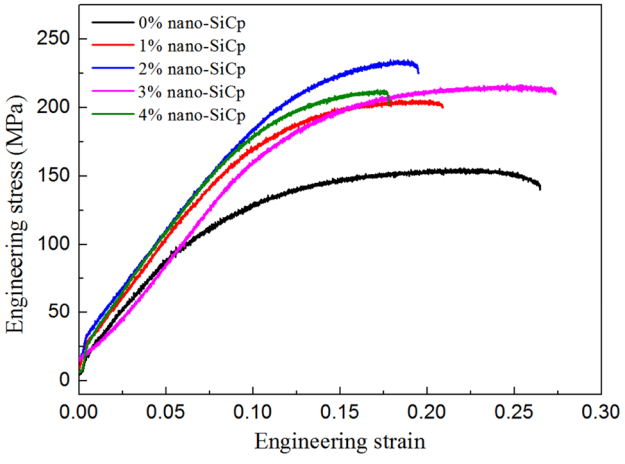

Figure 5: The engineering stress-strain curves of nanocomposites with different SiCp volume fractions.

significantly. However, when the addition amount of nano-SiCp is high, the distribution of nano-SiCp becomes worse, and some of the nano-SiCp aggregates, which reduces the number of effective nano-SiCp that plays the strengthening role, resulting in a decrease in the strength of the material. In addition, with the volume fraction of nano-SiCp increasing, the elongation of the composites decreases. This is because the addition of nano-SiCp increases the interface between SiCp and the aluminum matrix, and the interface is prone to crack initiation and expansion. Therefore, with the increase of nano-SiCp volume fraction, the elongation of nano-SiCp/Al–7Si matrix composites decreases gradually.

When the content of SiCp is 2%, the strength of the composites reaches the maximum value of 217 MPa and the results increased by 37.3% when compared with the Al–Si alloy without adding nano-SiCp. While the elongation is slightly lower than that of the Al–7Si alloy at this time, indicating that the SiCp/Al–7Si composites have better comprehensive properties. This may be because the nanoparticles have a smaller inter-particle distance, which is conducive to the dispersion strengthening effect of the reinforcement. In addition, there are more interfaces between nanoparticles and the matrix, and the binding effect on the matrix is stronger so that the tensile strength of nano-SiCp/Al–7Si matrix composites is increased obviously when compared with that of the Al–Si alloy.

Figure 7 shows the fracture morphology of nano-SiCp/Al–7Si composites with different SiCp volume fractions. It can be seen that there are a large number of irregularly distributed nests in the fracture of composites with different volume fractions, indicating that the fracture of composites is mainly due to the ductile fracture

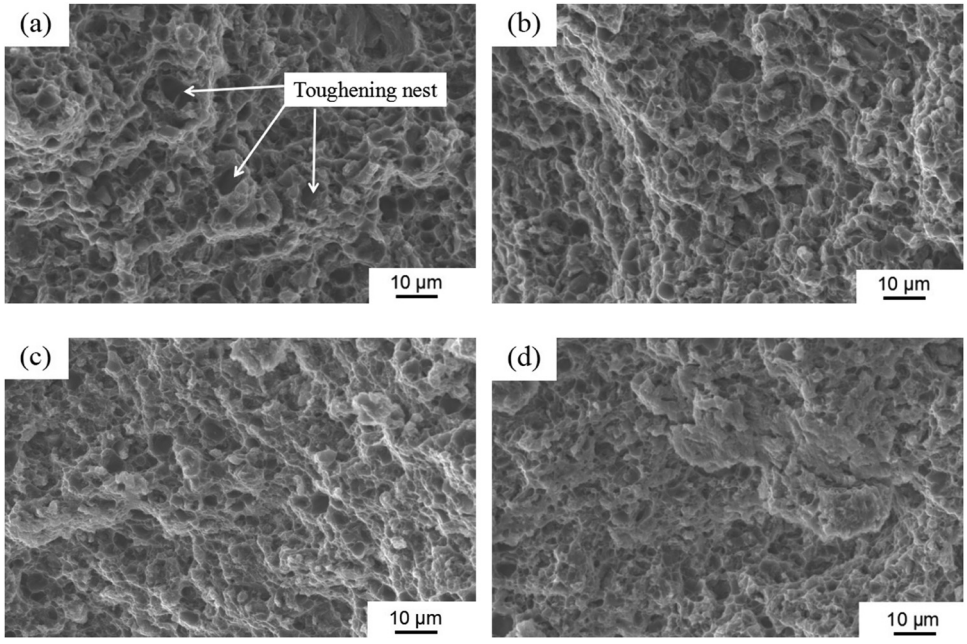

Figure 7: Fracture morphology of nanocomposites with different SiCp volume fractions: (a) 1% SiCp, (b) 2% SiCp, (c) 3% SiCp, and (d) 4% SiCp.

caused by the mechanism of microporous aggregation. The size of the toughening nest is different, the larger toughening nest is formed by the fracture or separation of Si particles in the matrix, and the smaller toughening nest is formed by plastic tearing of the matrix. In addition, it can be observed that with the increase of nano-SiCp content, the toughening nest depth in the fracture decreases, indicating that the ductility of the composites becomes worse, which is consistent with the results obtained from the tensile test.

3.3 Microstructure evolution during thermal deformation of nano-SiCp/Al–7Si composites

3.3.1 Microstructure of nano-SiCp/Al–7Si matrix composites at different deformation temperatures

Figure 8 is TEM images of the thermal deformation structure of 2% nano-SiCp/Al–7Si matrix composites at different thermal deformation temperatures and a strain rate of 5 s^{-1}. When the heat distortion temperature is 470°C, the corresponding TEM image is shown in Figure 8a, and it can be observed that there is a cellular substructure composed of high density in the composites. When the heat distortion temperature rises to 490°C, the corresponding TEM image is shown in Figure 8b. The dislocation density in the cellular substructure becomes less, and the cell wall gradually becomes clear. As shown in Figure 8c, when the heat distortion temperature is 510°C, the dislocation density in the cellular substructure of the composite material is further reduced, the cell wall becomes clearer, and subcrystals are gradually formed. Nano-SiCp is observed near the boundary, and the nano-SiCp may hinder the migration of the sub-grain boundary, thereby restricting the growth of the dynamic recovery subcrystal. When the heat distortion temperature is 530°C, the corresponding TEM image is shown in Figure 8d. There are two adjacent dynamic recovery subcrystals in the figure, and the internal dislocation density of the subcrystals is higher. Adjacent subgrains tend to merge into one grain gradually.

When the thermal deformation temperature is low, the degree of dynamic softening is limited, and the dislocations generated in the thermal deformation process form dislocation entanglement, thus forming a cellular substructure composed of high-density dislocations in the composites. With the thermal deformation temperature increase, the dislocation movement ability enhances. Therefore, the dislocations in the cellular substructure can be annihilated by cross-slip, so that the dislocations located in the cellular substructure are reduced or the dislocations move to the cell wall and arrange regularly on the cell wall by climbing, thus making the cell wall become clear and

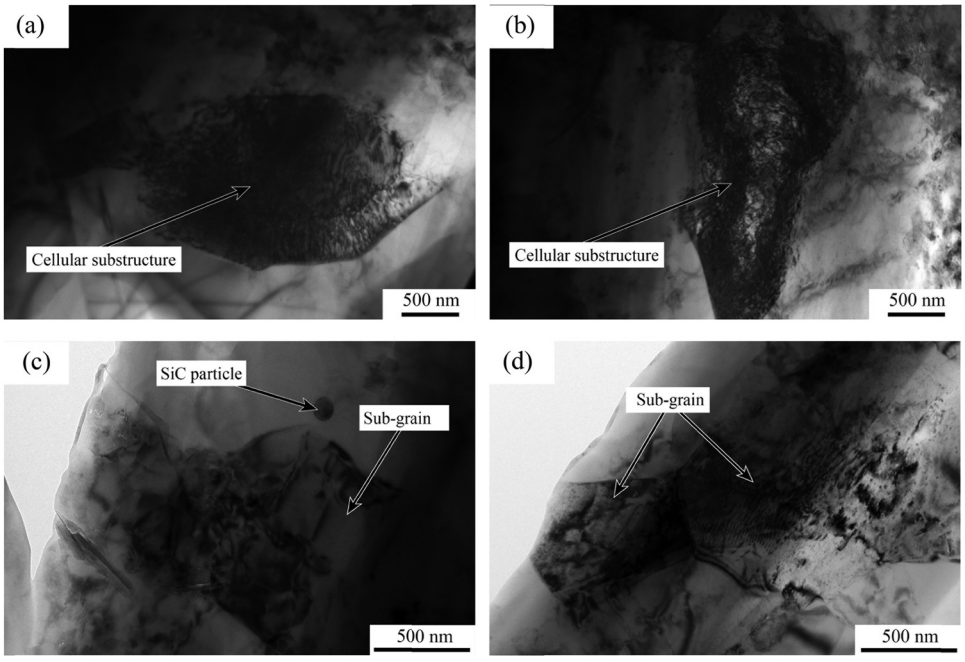

Figure 8: TEM images at strain rate of 5 s^{-1} and different deformation temperatures: (a) 470°C, (b) 490°C, (c) 510°C, and (d) 530°C.

gradually forming the subcrystals. With the further increase of deformation temperature, the migration ability of the sub-grain boundary is improved. Under the action of deformation storage, the dynamic recovery sub-crystals tend to merge.

3.3.2 Microstructure of nano-SiCp/Al–7Si matrix composites at different strain rates

When the deformation temperature is 530°C and the strain rate is different, the TEM images of the thermally

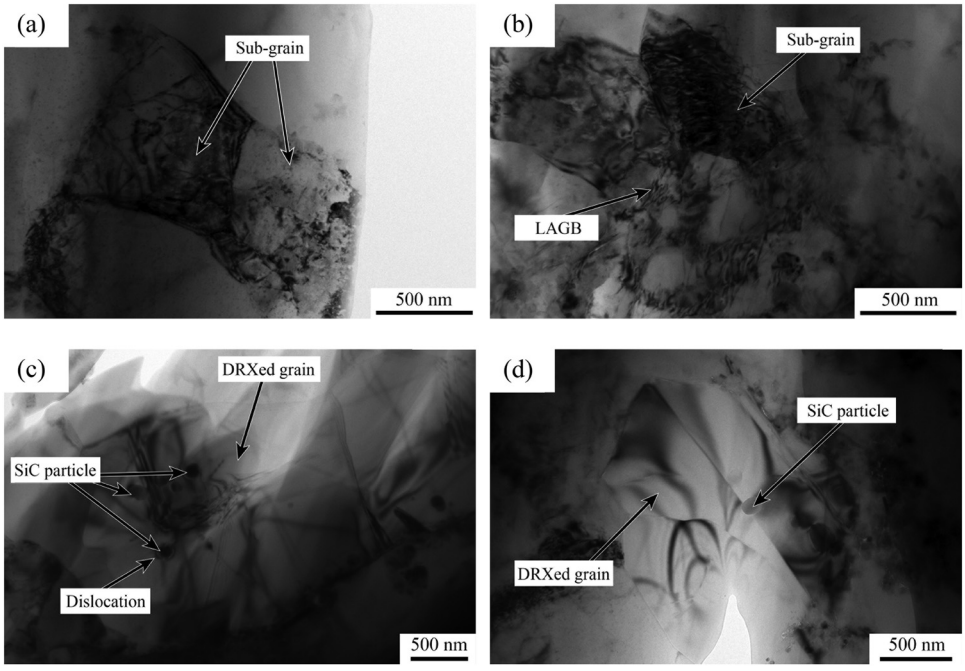

Figure 9: TEM images at different strain rate deformation and deformation temperature of 530°C: (a) 5 s^{-1}, (b) 1 s^{-1}, (c) 0.1 s^{-1}, and (d) 0.01 s^{-1}.

deformed structure are shown in Figure 9. When the strain rate is $5\,s^{-1}$ (Figure 9a), it can be observed that there are adjacent subcrystals with higher dislocation density in the composites, and the subcrystals tend to merge gradually. When the strain rate is $1\,s^{-1}$ (Figure 9b), the subgrain boundaries (LAGB) of the two adjacent subcrystals on the left become blurred and difficult to distinguish, indicating that the merger of sub-crystals has begun. The sub-grains in the upper right corner still contain more dislocations, indicating that the dynamic recovery has not yet been completed. As shown in Figure 9c, when the strain rate is $0.1\,s^{-1}$, distortionless crystal grains appear, and there are still some dislocations inside. It can also be observed that the dislocations bend at the nano-SiCp, and there are dislocation loops around part of the nano-SiCp. This indicates that the movement of the dislocation is blocked at the nano-SiCp, thereby bypassing the nano-SiCp. When the strain rate is $0.01\,s^{-1}$, the corresponding TEM image is shown in Figure 9d. There are undistorted equiaxed grains in the figure, the grain boundaries are straight and the dislocation density in the grains is relatively high, indicating that the dynamic recrystallization proceeds more fully. In addition, it can be noted that there are nano-SiCp near the dynamically recrystallized grains, and the nano-SiCp may hinder the migration of grain boundaries.

Under the condition of the same deformation temperature, when the strain rate is high, the deformation degree of the composites in the same time period is greater, the dislocation generation rate is accelerated, and the probability of dislocation tangles when the dislocation moves is also increased. In addition, the action time of the dynamic softening mechanism becomes shorter, which makes the dynamic softening mechanism cannot play an effective role. Therefore, there are still many dislocations in the composites when the strain rate is high. But when the composites are at a low strain rate, the dislocation generation rate reduces, making the probability of dislocation tangles in the process of sports decrease. In addition, dislocations have more time to climb and annihilate, and the grain boundaries also have more time migration. As a result, the dynamic softening is carried out more fully and the undistorted equiaxed grains appear in the composites.

3.3.3 Dynamic recovery mechanism of nano-SiCp/Al–7Si matrix composites

Figure 10a is the TEM image of the nano-SiCp/Al–7Si matrix composites at a deformation temperature of 470°C and a strain rate of $5\,s^{-1}$. There is a cellular substructure with a higher dislocation density in the figure. This is because under the conditions of low temperature and high strain rate, the dislocation generation rate and the probability of dislocations meeting during the movement become larger, and dislocation tangles are likely to occur

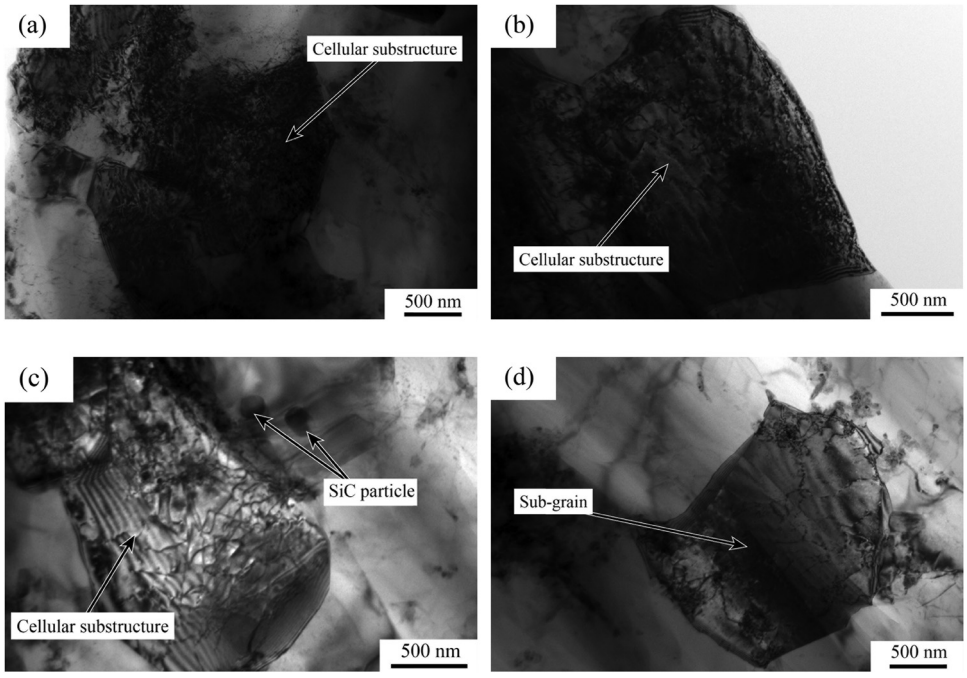

Figure 10: TEM images of nano-SiCp/Al–7Si matrix composites at different deformation conditions: (a) $T = 470$°C, $\dot{\varepsilon} = 5\,s^{-1}$; (b) $T = 470$°C, $\dot{\varepsilon} = 1\,s^{-1}$; (c) $T = 490$°C, $\dot{\varepsilon} = 5\,s^{-1}$; and (d) $T = 490$°C, $\dot{\varepsilon} = 1\,s^{-1}$.

during thermal deformation. At the same time, when the thermal deformation temperature is low, the dislocation cross-slip ability is weak, and the vacancy concentration is also low, which is not conducive to the climbing motion of the edge dislocation. Therefore, the dislocation cross-slip is mainly used to achieve dynamic softening under this condition. Figure 10b is a TEM image of the nano-SiCp/Al–7Si matrix composites at a deformation temperature of 470°C and a strain rate of $1\,s^{-1}$. The dislocation density in the cellular substructure reduces with the strain rate decreases. As the deformation speed becomes slow, the dislocation generation rate and the probability of dislocations meeting during the movement are reduced. The effect of dislocations annihilate through cross-slip is more significant, thereby reducing the dislocations in the cellular substructure. As shown in Figure 10c, when the thermal deformation temperature is 490°C and the strain rate is $5\,s^{-1}$, the vacancy density in the composites increases with the deformation temperature increases, thereby increasing the ability of dislocation climbing. The dislocations that move to the cell wall through cross-slip movement are regularly arranged on the cell wall by climbing so that the cell wall gradually becomes clear, when the thermal deformation temperature is 490°C and the strain rate is $1\,s^{-1}$ (Figure 10d). The three-dimensional dislocation network within the substructure is gradually untangled, some dislocations are annihilated by cross-slip movement. Part of the dislocations move to the cell wall and are arranged regularly at the cell wall by climbing, and clear sub-grain boundaries appear, thereby forming sub-crystals. Therefore, when the deformation temperature is low and the strain rate is high, the intracellular dislocation density is mainly reduced by the dislocation cross-slip. After the deformation temperature is increased or the deformation rate is reduced, the dynamic recovery of the composites realizes the dynamic softening through the unwinding of the three-dimensional dislocation network, dislocation cross-slip, and climbing.

3.3.4 Dynamic recrystallization mechanism of nano-SiCp/Al–7Si matrix composites

In Figure 11a, it can be seen that there are still two adjacent subcrystals with a certain density inside, and the grain boundary of the two subcrystals has become blurred. This is because the dislocations on the adjacent sub-grain boundaries of the two subcrystals move to other surrounding sub-grain boundaries, the dislocation density on the sub-grain boundaries gradually decreases so that the adjacent sub-grain boundaries become blurred until the sub-grain boundary disappeared. At the same time, due to more dislocations existing on the surrounding sub-grain boundaries, the crystal difference between these two sub-crystals and other adjacent sub-crystals increases, thereby transforming large-angle grains gradually and forming dynamic recrystallization nuclei. This situation corresponds to the sub-crystal merging mechanism. Figure 11b is the TEM image of the nano-SiCp/Al–7Si composites at another position when the deformation temperature is 530°C and the strain rate is $1\,s^{-1}$. It can be seen that there is a big difference in the number of dislocations in the subcrystals on both sides of the high-angle grain boundary (HAGB). The high-angle grain boundary tends to gradually migrate to the sub-crystal containing more dislocations. As a result, subcrystals with a higher dislocation density are absorbed to form distortion-free crystal grains. This situation corresponds to the grain boundary bowing mechanism. Subsequently, under the action of the deformation storage energy, the large-angle grain boundary tends to gradually deviate from the center of curvature and migrate to the surrounding distorted grains, and then, the dynamic recrystallized grains grow up.

4 Conclusions

This study takes nano-SiCp/Al–7Si composites prepared by powder metallurgy as the research object. With the

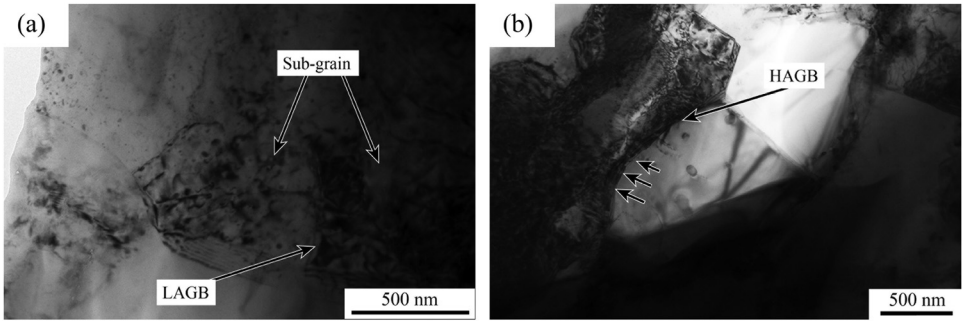

Figure 11: TEM images of nano-SiCp/Al–7Si matrix composites at deformation temperature of 530°C and strain rate of $1\,s^{-1}$.

help of advanced microstructure characterization techniques and performance analysis methods, the effect of nano-SiCp volume fraction on the microstructure and properties of composites is systematically studied. Based on optimizing the volume fraction of nano-SiCp, the thermal deformation behavior of the composites is investigated. The results obtained are as follows:

(1) When the volume fraction of nano-SiCp is low, the distribution of nano-SiCp is more uniform. With the increase of nano-SiCp content, the distribution uniformity of nano-SiCp is gradually decreased. Because the surface of nano-SiCp is easy to absorb gas and the agglomeration and distribution of nano-SiCp is not conducive to the sintering process, the density of the composites decreases gradually with the increase of nano-SiCp content.
(2) With the increase of nano-SiCp content, the hardness of the composites tends increasing gradually, and the increased amplitude gradually decreases. Due to the addition of nano-SiCp, there are many interfaces between SiCp and Al matrix, and cracks are prone to initiation and expansion at the interface. Therefore, as the volume fraction of nano-SiCp increases, the elongation of nano-SiCp/Al–7Si composites gradually decreases. When the addition amount of nano-SiCp is small, nano-SiCp can not only hinder the slip of dislocations but also induce the initiation of a large number of dislocations in the matrix, thus significantly strengthening the material. However, when the addition amount of nano-SiCp is high, some of the SiCp will aggregate, resulting in a decrease in the strength of the material. When the nano-SiCp content is 2%, the strength of the composites reaches the maximum value of 217 MPa. Compared with the Al–Si alloy without adding nano-SiCp, the results increased by 37.3%.
(3) As the strain rate decreases and the deformation temperature increases, the dislocation density in the composite material gradually decreases and the dynamic softening progresses more fully. The dynamic recrystallization nucleation mechanism mainly includes the subcrystal merging mechanism and the grain boundary bowing mechanism.

Acknowledgments: The authors are grateful for the financial support from the National Natural Science Foundation of China (grant no. 51771070).

Funding information: This research has been funded by the National Natural Science Foundation of China (grant no. 51771070).

Author contributions: For this article, A. Wang and J. Xie conceived and designed the preparation method and follow-up experiment content of nano-SiCp-reinforced Al matrix composites. Z. Wang performed the experiment. X. Dong conducted the data analysis and wrote the manuscript. The authors applied the SDC approach for the sequence of authors. All authors have accepted responsibility for the entire content of this manuscript and approved its submission.

Conflict of interest: The authors declare no conflict of interest.

Data availability statement: All data generated or analyzed during this study are included in this published article.

References

[1] Lin H, Guo X, Song K. Synergistic strengthening mechanism of copper matrix composite reinforced with nano-Al_2O_3 particles and micro-SiC whiskers. Nanotechnol Rev. 2021;10(1):62–72.
[2] Liu Y, Yang C, Chen W. Effects of particle size and properties on the microstructures, mechanical properties, and fracture mechanisms of 7075Al hybrid composites prepared by squeeze casting. J Mater Sci. 2014;49(22):7855–63.
[3] Gao X, Zhang X, Qian M. Effect of reinforcement shape on fracture behaviour of SiC/Al composites with network architecture. Compos Struct. 2019;215:411–20.
[4] Liu Q, Wang F, Wu W. Enhanced mechanical properties of SiC/Al composites at cryogenic temperatures. Ceram Int. 2019;45(3):4099–102.
[5] Ye T, Xu Y, Ren J. Effects of SiC particle size on mechanical properties of SiC particle reinforced aluminum metal matrix composite. Mater Sci Eng A. 2019;753:146–55.
[6] Mao Q, Xu X, Jiang Z. Effect of SiCp volume fraction on microstructure and properties of powder metallurgy SiCp reinforced aluminum matrix composites. Mater Res Exp. 2019;6(10):1065a3.
[7] Wang A-Q, Tian H-W, Xie J-P. Properties investigation and microstructures characterization of SiCp/6061Al composites produced by PM route. IOP Conf. 2018;292:012055.
[8] Bembalge OB, Panigrahi SK. Influence of SiC ceramic reinforcement size in establishing wear mechanisms and wear maps of ultrafine grained AA6063 composites. Ceram Int. 2019;45(16):20091–104.
[9] Monazzah AH, Pouraliakbar H, Bagheri R. Al-Mg-Si/SiC laminated composites: Fabrication, architectural characteristics, toughness, damage tolerance, fracture mechanisms. Compos Part B. 2017;125:49–70.
[10] Li J, Lü S, Wu S. Effects of nanoparticles on the solution treatment and mechanical properties of nano-SiCp/Al-Cu composites. J Mater Process Technol. 2021;296(2):117195.

[11] Hasan T. Mechanical properties of nanomaterials: a review. Nanotechnol Rev. 2020;9(1):259–73.
[12] Mousavian RT, Behnamfard S, Khosroshahi RA. Strength-ductility trade-off via SiC nanoparticle dispersion in A356 aluminium matrix. Mater Sci Eng A. 2020;771:138639.
[13] Wang L, Qiu F, Zou Q. Microstructures and tensile properties of nano-sized SiCp/Al-Cu composites fabricated by semisolid stirring assisted with hot extrusion. Mater Charact. 2017;131:195–200.
[14] Zhang L-J, Qiu F, Wang J-G. High strength and good ductility at elevated temperature of nano-SiCp/Al2014 composites fabricated by semi-solid stir casting combined with hot extrusion. Mater Sci Eng A. 2015;626:338–41.
[15] Hu K, Yuan D, Lü S. Effects of nano-SiCp content on microstructure and mechanical properties of SiCp/A356 composites assisted with ultrasonic treatment. Trans Nonferrous Met Soc China. 2018;28(11):2173–80.
[16] Kamrani S, Riedel R, Seyed, Reihani SM. Effect of reinforcement volume fraction on the mechanical properties of Al–SiC nanocomposites produced by mechanical alloying and consolidation. J Compos Mater. 2010;44(3):313–26.
[17] Chen S, Fu D, Luo H. Hot workability of PM 8009Al/Al_2O_3 particle-reinforced composite characterized using processing maps. Vac. 2018;149:297–305.
[18] Wang C, Zhang L, Wei S. Preparation, microstructure, and constitutive equation of *W*–0.25 wt% Al_2O_3 alloy. Mater Sci Eng A. 2019;744:79–85.
[19] Gangolu S, Rao AG, Sabirov I. Development of constitutive relationship and processing map for Al-6.65Si-0.44Mg alloy and its composite with B_4C particulates. Mater Sci Eng A. 2016;655:256–64.
[20] Wang Z, Wang A, Xie J. Dynamic softening mechanism of 2 vol% nano-sized SiC particle reinforced Al-12Si matrix composites during hot deformation. Mater Res Express. 2020;7(8):086520.
[21] Shu S-W, Jian Y-L, Ping A. Particle distribution and mechanical properties of nano-SiCp/Al-Cu composites. Mater Sci Forum. 2018;941(3):2060–5.
[22] Mohanavel V, Kumar SS, Mariyappan K. Mechanical behavior of Al-matrix nanocomposites produced by stir casting technique. Mater Today: Proc. 2018;5(13):26873–7.
[23] Abdullahi K, Al-Aqeeli N. Mechanical alloying and spark plasma sintering of nano-SiC reinforced Al-12Si-0.3Mg alloy. Arab J Sci Eng. 2014;39(4):3161–8.
[24] He G, Li W. Influence of nano particle distribution on the strengthening mechanisms of magnesium matrix composites. Acta Mater Comp Sin. 2013;30(2):105–10.
[25] Levy-Tubiana R, Baczmanski A, Lodini A. Relaxation of thermal mismatch stress due to plastic deformation in an Al/SiCp metal matrix composite. Mater Sci Eng A. 2003;341(1–2):74–86.